University of Maryland GEOL394H

Characterizing carbon sources and quality in four Baltimore streams with fluorescence spectroscopy

Author:
Grant JIANG

Advisor:
Dr. Sujay Kaushal

1 Abstract

Globally, riverine inputs are one of the largest external sources of carbon to the oceans (Doney, 2010). In the Washington/Baltimore metropolitan area, many of the local watersheds drain into the Chesapeake Bay, which has experienced decades of eutrophication (Boesch et al., 2001). Originally thought to be a non-reactive byproduct of biological activity, the effects of readily reactive, or labile, organic matter on aquatic chemistry have become better understood with advances in fluorescence spectroscopy. Aquatic dissolved organic carbon serves as a food source for heterotrophic bacteria, contributes to freshwater acidity, and serves as a vector for contaminants. A novel approach combining excitation emission matrix fluorescence spectroscopy, parallel factor analysis (PARAFAC) and fluorescence indices was used to investigate the sources and quality of organic carbon in four small Baltimore streams via their optical properties. The results suggest that end-member sources of organic carbon could be characterized by their optical properties. Differences not immediately apparent from visual inspection of excitation emission matrices were resolved through the application of fluorescence indices and PARAFAC. Furthermore, a hydrological control is suggested to govern sources of DOC into these four streams. Two terrestrial humic-like components and one non-humic component were identified by PARAFAC, and a discussion on potential implications is provided. A thorough introduction and methodology is also included.

Contents

T	Abstract	1			
$\mathbf{C}\mathbf{c}$	ontents	2			
2	Introduction2.1 Fluorescence Spectroscopy2.2 Hypotheses	3 4 6			
3	Methodology 3.1 Site Descriptions	7 7 7 7 8			
4	Data4.1 Data Collection	10 10 11 11 11 11 12			
5	Results and discussion5.1 End member EEMs5.2 Fluorescence Indices5.3 PARAFAC results	13 13 16 20			
6	Directions for future work				
7	Conclusions 7.1 Potential for tracking natural vs. anthropogenic sources of DOC in streams . 2 7.2 Hydrologic variability drives sources and quality of DOC exported to streams . 2 7.3 DOC components in forested and urban streams				
8	Acknowledgements 25				
9	Bibliography 2				
10	Appendix I				

2 Introduction

With the development of modern energy systems, chemical industries, and mass agriculture, ever growing fluxes of nutrients are released - advertently or inadvertently - into the environment (Doney, 2010). In urban watersheds, this problem is compounded by the replacement of natural drainage systems with infrastructure such as storm drains, gutters, and sewage pipes, increasing the efficiency of transport to urbanized streams (Kaushal and Belt, 2012). Within the next two decades, 60% of the world's population is expected to live in cities, with a disproportionally high percentage of the population concentrated near coastlines. As population and urbanization increase, the combined impact of climate and land usage on the sources and quality of organic carbon delivered to coastal zones become of particular interest.

In forested streams, ecological functions are defined by adjacent riparian zones, which regulate the heat budget and supply organic matter to aquatic food webs. In urbanized streams, headwater and riparian zones are expanded by hydrologic connectivity with impervious surfaces, greatly increasing surface area for accumulation, storage, and transport of organic matter (Kaushal and Belt, 2012). Increased organic carbon loads in urbanized streams may result in more heterotrophic and polluted downstream tributaries. Due to allochthonous contributions, streams and rivers can be heterotrophic in nature; a heterotrophic system entails that the primary form of metabolism is consumption of bioavailable carbon rather than autochthonous production through photosynthesis.

Organic matter exists as dissolved, colloidal, and particulate forms in natural waters, with the dissolved fraction being the most studied fraction (Hudson et al., 2007). With the exception of running waters containing high concentrations of organic particles or extreme algae blooms, dissolved organic carbon (DOC) is a dominant form of organic matter in the majority of aquatic ecosystems (Findlay and Sinsabaugh, 1999). Terrestrial inputs from soils and leaf litter comprise the large sources of organic matter to streams, serving as food for heterotrophic bacteria. The labile fraction of DOC available for microbial consumption is referred to as bioreactive dissolved organic carbon, or BDOC. Bacteria further convert BDOC into organic acids, increasing water acidity. Toxic trace metals and other pollutants also adsorb onto the surfaces of bulk organic matter, facilitating transport downstream. Autochthonous, or *in-situ* sources of DOC are typically attributed to carbon generated from primary producers such as benthic algae (Findlay and Sinsabaugh, 1999).

The multitude of possible sources and pathways that DOC may take results in vastly heterogeneous and complex chemical structures. It is thus not possible to assign even broad compositional categories to DOC (Findlay and Sinsabaugh, 1999). A number of bulk measurement techniques, however, have thus been used to study DOC in aquatic systems, focused on characterizing DOC by operational classifications rather than by chemical compositions. In the last two decades, fluorescence spectroscopy has emerged as a vital technique to investigate the composition, concentration, and dynamics of organic carbon in both marine and aquatic environments.

Using fluorescence spectroscopy, I characterized variations in carbon sources and quality in four small Baltimore area streams. These four streams are monitored as a part of the Baltimore Ecosystem Study, and data are collected and analyzed in Dr. Sujay Kaushal's lab here at the university. The streams represent a gradient of land use, with two forested

and two urbanized streams. I analyzed the fluorescence patterns of end-member sources of DOC and compared them to stream fluorescence data using fluorescence indices and parallel factor analysis.

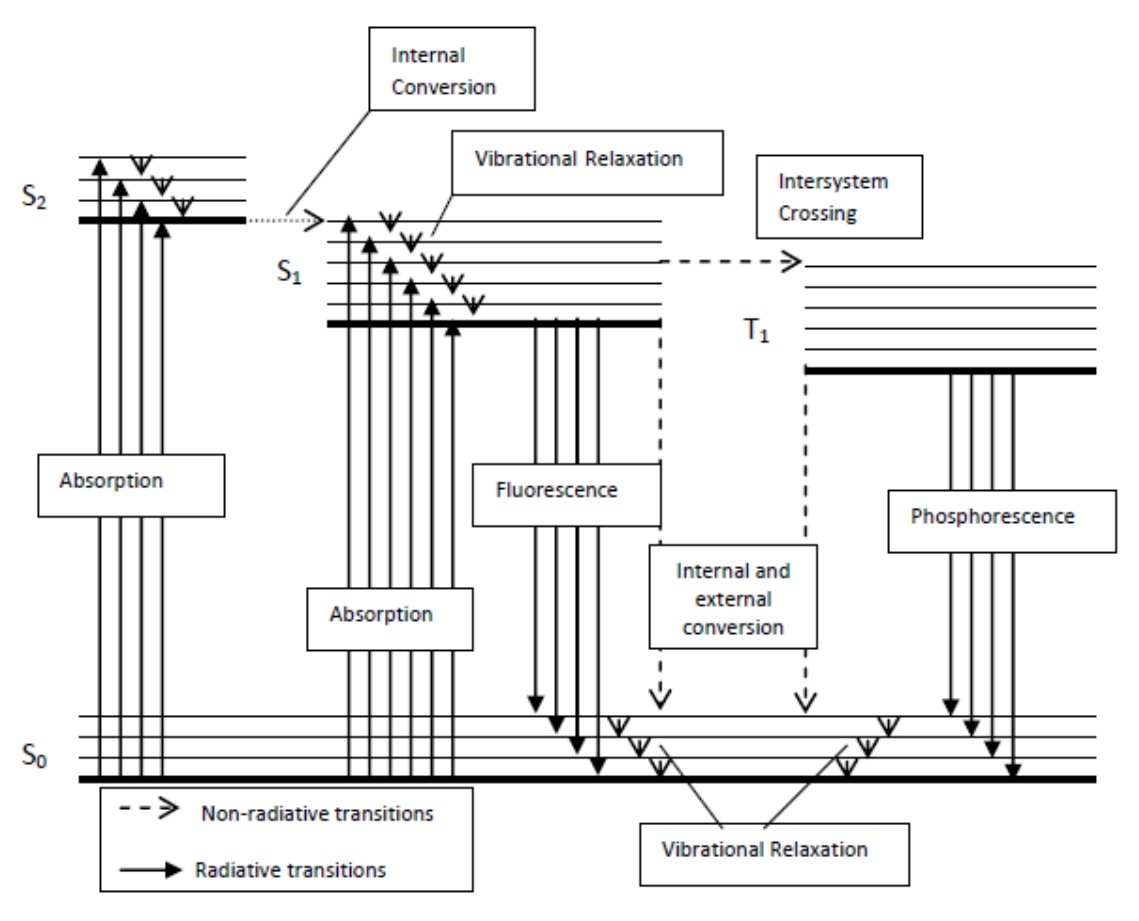


Figure 1: A Jablonski diagram. Vibrational states are denoted with S*, and the arrows denote possible pathways taken by the electrion. Adapted from Skoog et al. (2007)

2.1 Fluorescence Spectroscopy

Molecules absorb ultraviolet and visible radiation by undergoing vibrational and electronic excitation. Some of this absorbed energy is reemited as radiation, and some is given off as heat to the solvent. The emitted radiation in these processes is referred to as photoluminescence. Specific luminescence phenomena are fluorescence and photoluminescence; the former forms the basis of fluorescence spectroscopy. Electronic and vibrational transitions are typically described with a photoluminescent energy level diagram, commonly known as a Jablonski diagram (Figure 1).

Absorption of radiant energy - a photon - by an electron raises its energy to an excited state S*. From this state, the spins of the two electrons are paired (opposing), as per the Pauli Exclusion Principle (Skoog et al., 2007). Relaxation to the ground state may occur by a radiation-less process known as internal conversion, followed by reemission of a photon – resulting in fluorescence.

Alternatively, the electron may crossover to an excited triplet state from the excited singlet state in a process known as intersystem crossing. In the triplet state, the spin orientation of the excited electron is flipped and the spins of the electron pair become parallel. Transitions from the triplet state to singlet state are unfavorable and thus much less probable, making phosphorescence a much slower process than fluorescence.

Fluorescence is measured using a spectrofluorometer, which uses diffraction grated monochromators to isolate the wavelengths of incident and fluorescent light. The wavelengths at which photon absorbance, excitation, and emission occur are specific to the fluorescing molecule (Hudson et al., 2007). Compounds that absorb light are known as chromophores, and fluorescent compounds are known as fluorophores. The efficiency of a photoluminescent reaction is defined as the quantum yield:

$$\Phi = \frac{\text{\# of photons emitted}}{\text{\# of photons absorbed}}$$

Fluorescence studies on aquatic environments are focused on the mixture of poorly defined heterogeneous compounds that comprise the fluorescent fraction of dissolved organic matter. Aromatic organic compounds are particularly well suited to fluorescence studies due to delocalized electrons present in compounds with alternating single and multiple bonds – a structure seen in benzene rings (Hudson et al., 2007). Benzene rings are thus the primary fluorescent moieties in organic compounds, and their ubiquitous presence in DOC is what makes fluorescence spectroscopy so applicable to the characterization of DOC. Unbound electrons in oxygen atoms, most often found in ketone or aldehyde groups, also participate in fluorescence. Oxygen in carboxylic groups may also participate, but their contribution is negligible compared to ketone and aldehyde groups (Skoog et al., 2007).

Due to the difficulty in precisely identifying the composition of fluorescent DOC, fluorophores with the same optical properties as idealized, model substances from the International Humic Substances Society (IHSS) are named fulvic-like, humic-like, and protein-like, respectively. Some idealized fluorophores are presented in figure 2.

Humic substances are the most commonly studied fluorophores. Complex and vastly heterogeneous mixtures formed by biochemical and chemical reactions during the decay of organic matter, humic substances comprise about 50% of the DOC in aquatic systems (IHSS, 2007). Humic substances can further be sub-divided into three categories, defined by their solubility at different pH level: fulvic acids, humic acids, and humins. Fulvic acids are soluble in water of any pH, humic acids are insoluble at pH lower than 2, and humins are water-insoluble at any pH (Hudson et al, 2007; IHSS, 2007). In water, idealized fulvic and humic acids behave as diprotic or triprotic acids, due to the presence of carboxyl (-COOH) and/or phenol (-C₆H₅OH) groups (Ritchie and Perdue, 2003).

Three amino acids (tryptophan, tyrosin, phenylalanine) are also commonly studied due to their aromatic nature, and are present in proteins and peptides. Tryptophan typically has the strongest fluorescence intensity due to its high quantum yield, and is an essential amino acid; this means that it cannot be synthesized by an organism and must be part of its diet. These amino acids are associated with protein fluorescence, and point to the presence of bioavailable DOC.

These fluorophores can be characterized due to advances in fluorescence spectroscopy.

Excitation, emission, and fluorescence intensity can be scanned over a range of wavelengths synchronously. These data sets, known as excitation emission matrices (EEMs), can be plotted on a single figure, thus developing a map of "optical space". Within these plots, fluorophores can be identified by the location of their maximum fluorescence in optical space. The ratio of fluorescence intensity at one location to another can provide indices describing the properties of bulk fluorescent material (Coble, 1996; Zsolnay et al., 1999; Mcknight et al., 2001; Huguet et al., 2009).

Structure of tryptophan, tyrosine, phenylalanine

Theoretical humic acid Stevenson, (1982) cited in Aitken et al., (1985)

Theoretical fulvic acid Buffle, (1977) cited in Aitken et al., (1985)

HOOC
$$CH_2$$
 CH_2 CH_3 CH_2 CH_2 CH_3 CH_2 CH_2 CH_3 CH_2 CH_3 CH_4 CH_5 CH_5 CH_6 CH_6 CH_7 CH_8 CH_8 CH_8 CH_8 CH_9 CH

Figure 2: Ideal theoretical structures of common aquatic fluorophores, adapted from Hudson et al. (2007).

2.2 Hypotheses

I made two hypotheses at the start of my thesis project – the first, that end-member sources of DOC can be differentiated from each other via fluorescence spectroscopy, and that the optical properties of each source will change over time. Secondly, that urban streams will

have DOC originating from urban sources, and forested streams will have DOC originating from forested, or "natural" sources. The accompanying null hypothesis is that both urban and forested streams receive the same type of DOC inputs.

3 Methodology

As a part of the Baltimore Ecosystem Study (BES), researchers monitor a number of streams in the Baltimore metropolitan area. These streams range in drainage area and represent a range of land use gradients: from forested, agricultural, to heavily urbanized. Biweekly water samples are taken and analyzed in Dr. Sujay Kaushal's laboratory. My project examined the sources and transformations of carbon in four small watersheds, two urban and two forested. The urban sites are contained in the Gwynns Falls watershed, the primary focus of the BES program. The forested sites are located in Oregon Ridge State Park and in the Gunpowder Falls watershed, adjacent to Gwynns Falls.

3.1 Site Descriptions

3.1.1 Urban Streams

- i. Dead Run is an urban stream draining an area of 5.52 mi², and is located 0.31 miles west of Baltimore City limits, 1.2 miles southwest of Woodlawn. The USGS gauge is located at 39°18'40.4",76°42'59.9", about 2.5 miles upstream of the mouth. Parking is available on Kernan Dr, on a strip of gravel next to "No Parking on Grass" sign. About 41% of the watershed is impervious. USGS station number 01589330.
- ii. Gwynns Run is a small tributary contained of Gwynns Falls with a drainage area of 2.5 mi². The sampling site is located at 39°16′41.3″,76°39′07.2″, below I-93 and next to the Carroll Park golf course. Gwynns Run feeds into the larger Carroll Park branch of Gwynns Falls, and is a target of efforts to improve water quality and sewer infrastructure in the city of Baltimore. This watershed contains over 65% impervious surfaces. USGS station number 015835180.

3.1.2 Forested Streams

- iii. Baisman Run is located in Oregon Ridge State Park, draining 1.47 mi². The sampling site is located at 39°28′46.1″,76°40′40.9″, 0.6 miles southwest of Broadmoor and 0.3 miles upstream from the mouth. The gauging station is directly below a small footbridge, off of Ivy Hill Rd. This site is about 80% forest and 20% surburban residential developments.USGS station number 01583580. This site is about 80% forest and 20% surburban residential developments.
- iv. Pond Branch is located further up Ivy Hill Rd. and inside Oregon Ridge State Park, draining 0.12 mi². The gauging station is located at 39°28'49.1",76°41'15.0", about 2.3 miles west of Cockeysville. Pond Branch is 99% forest. USGS station number 01583570.

None of the streams receive point inputs, and all but Gwynns Run are continuously monitored for discharge. Discharge at Gwynns Run can be approximated by an empirical relationship with discharge at Carroll Park. Soil at the forested sites is very fine-grained, brown, and clay-like in appearance, while soil at the urban sites is coarser-grained, and darker. The urban streams have very little natural drainage networks, and are fed largely by runoff. Figure 3 is a map of the location of the four streams.

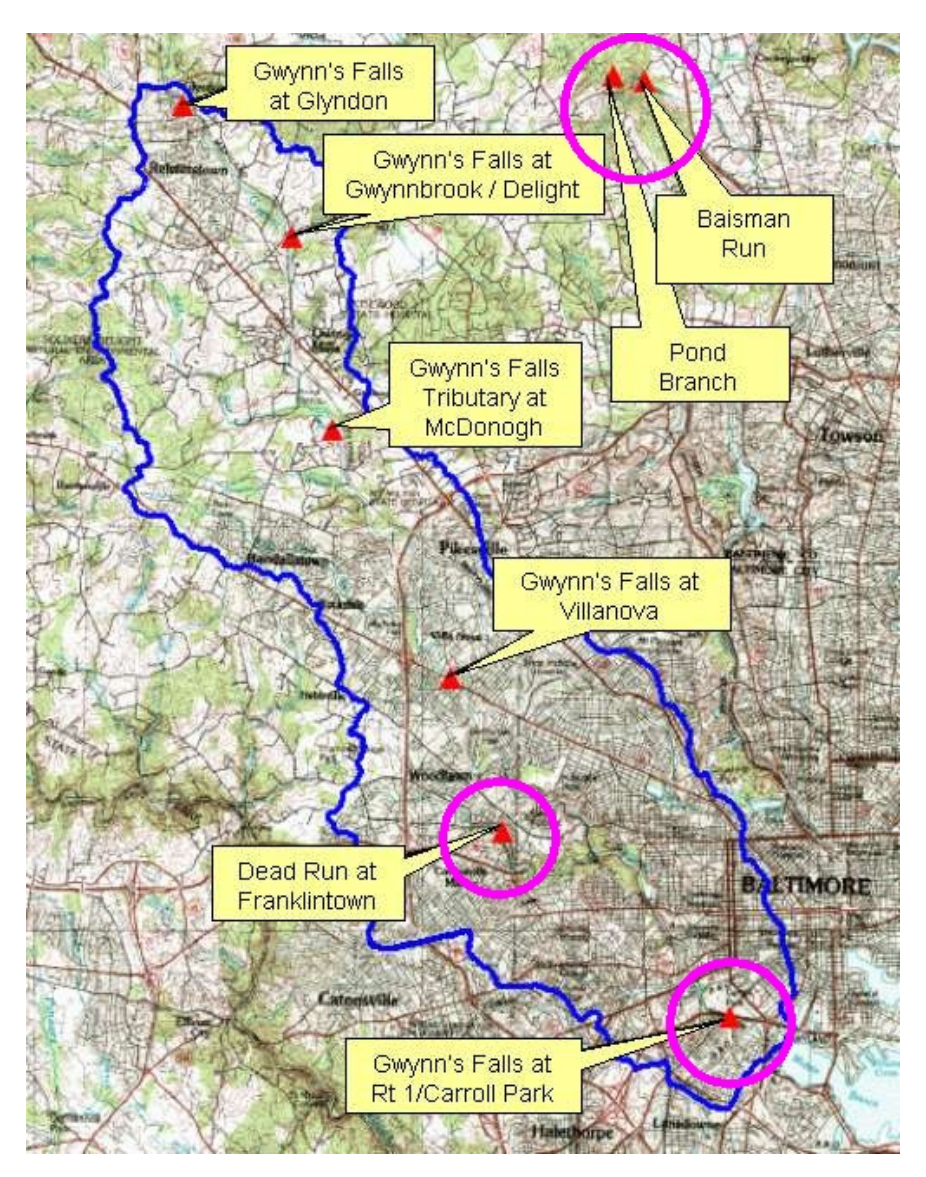


Figure 3: Map of the four streams monitored as part of the BES program. Image courtesy of the BES website (http://beslter.org).

3.2 End-member fluorescence analysis

To characterize DOC sources to these four streams, I first identified the four most likely and most major sources of organic carbon to watersheds: two anthropogenic and two natural

sources. Untreated sewage and storm drain runoff comprise the former; decaying organic matter in the form of leaf litter and algae comprise the latter. The forested sources were chosen for their ubiquity – leaf litter and algae are present in all four streams. Stormwater runoff was chosen as the city of Baltimore and its suburbs are heavily urbanized, leading to large percentages of impervious surfaces. Storm drains in the city of Baltimore drain directly from the road, or parking lots. Baltimore county is also home to an aging septic system, and concerns have risen over sewage leaks. Furthermore, Kaushal and Belt (2012) noted that Oregon Ridge State park is adjacent to a number of residential developments and accompanying septic systems. As sewage contains readily consumable organic carbon and is a perfect candidate for microbial humification, a soil sample was also taken to ensure that the two sources had different optical properties.

Next, I made a plan to conduct seasonal sampling to account for seasonal variation in sources of DOC. Raw sewage, for instance, should display stronger protein-like fluorescence characteristics in the summer, when flow is lowest and temperature is highest – ideal for microbial heterotrophy. The signature of decaying organic matter would be strongest in the fall and early winter, when leaves fall off deciduous trees into or near streams. Contributions from primary productivity come from algae and would be highest in the early spring, when the region's watersheds experience seasonal algal blooms. Contributions from storm drain runoff would be dependent on precipitation, a stronger signal in the streams would be expected in late autumn during hurricane season, or in early spring from snowmelt.

While there has been some work done on the fluorescence characteristics of algae and decaying organic matter, the optical properties of anthropogenic carbon are relatively unstudied. This is complicated as the optical properties of storm drain, or urban, runoff may vary from region to region, depending on the septic and storm drainage systems present. I conducted sampling in fall, winter, and spring to capture seasonal variations in these end-member sources. I was not able to conduct summer sampling due to time limitations.

Dr. Shuiwang Duan conducted preliminary studies on the optical properties of leaf litter, and found that the optical properties varied slightly depending on tree species. To account for this, I collected available leaf litter in the region immediately around (; 0.5m) each stream. Three groups of leaf litter were collected: Dead Run, Gwynns Run, and Oregon Ridge; the latter corresponds with both Pond Branch and Baisman Run. Leaf samples were first dried in an oven at room temperature for approximately 48 hours, then leached into Millipore water for 24 hours at a concentration of 1g/mL. Leaf litter was only present during fall and winter sampling, and I took care to only pick leaf litter from the top-most layer of leaf litter.

Algal material was collected from rocks encrusted with brown filamentous algae in the fall and winter. The algal bloom during spring sampling allowed me to collect algae directly from the stream itself; the optical properties were largely identical between rock-encrusting and free-floating algal samples. After collection, the algae was dried in an oven at room temperature for 48 hours, then leached into Millipore water at a concentration of 1g/mL. In the case of the rock-encrusting samples, the algae was first scraped off the rock with a sterile scalpel.

Storm drain runoff was collected from a storm drain located next to the Carroll Park gauging station, below I-93. This drain drains directly from the nearby streets, primarily Washington Boulevard. Sewage samples were obtained from Back River Wastewater Treatment Plant, located at 8201 Eastern Avenue. The plant is located at the west shore of Back

River and receives influent from a number of the region's watersheds, including Gwynns Falls.

A soil sample was also taken from the bank Dead Run sampling site during winter sampling, 0.5m away from the stream and 1.5m down. Soil was only collected in Oregon Ridge and Dead Run as the soil at Gwynns Run was protected by a mesh fencing, and a thick layer of boulders. Soil from Oregon Ridge was not analyzed, due to its almost clay-like consistency. To extract water soluble organic carbon from the Dead Run sample, samples were prepared in the style of Boyer and Groffman (1996): 75g of soil was weighed into a 0.5L Mason jar, to which 300 mL of Millipore water was added. The Mason jar was then sealed with Parafilm, and placed on a shaker table over night. The extract was then decanted, centrifuged at 10,000 rpm for 15 minutes, and filtered.

Autumn sampling occurred on October 28, 2012; winter sampling on January 27, 2013; spring sampling on March 19, 2013. During each sampling trip, all four end-member sources were collected in a single day. After collection, samples were filtered through a 0.7 micron ashed glass microfiber filter, then within two weeks, fluoresced on the Horiba Jobin-Yvon FluoroMax-4 spectrofluorometer located in Dr. Kaushal's lab. Property safety measures were taken when handling sewage samples.

Before analysis, fluorescence samples are typically diluted to a low absorbance († 0.1) to account for an inner filter effect. This was done for winter and spring end-member samples, but not for the fall end-member samples nor for the BES samples. BES samples are not corrected for absorbance, and I fluoresced my fall samples under the assumption that absorbance correction was unneeded. However, Rose Smith conducted an experiment comparing absorbance corrected samples and uncorrected samples and found the difference to be less than 2%. Furthermore, by Beer-Lambert's law, the largest impact of not correcting for absorbance is the maximum intensity of fluorophores – the location of the peaks in optical space remains unchanged, and the changes in maximum intensity are proportional to absorbance (Huguet et al., 2009). That is, a higher or lower maximum intensity would result in proportional changes throughout the analysis.

4 Data

4.1 Data Collection

Data were collected in ratio mode (signal/reference) at excitation wavelengths of 240 to 450nm at intervals of 5nm, and emission wavelengths of 300 to 600nm at intervals of 2nm. Each end-member samples were fluoresced at least twice to account for instrument error. Resulting excitation emission matrices (EEMs) were then corrected to a daily Millipore water blank. The analytical uncertainty associated with each individual sample was less than 2%.

Forty-one total BES samples were analyzed for my thesis, from September 05, 2012 to March 8, 2013 in roughly biweekly intervals. Twenty-one of the samples came from urban streams, and twenty samples came from forested streams. There are no data between September 20, 2012 and October 31, 2012, as the spectrofluorometer was inoperative. Each BES stream sample was only fluoresced once; overall analytical uncertainty is expected to

be less than 2%.

4.2 Data Analysis

After data were collected, blank and instrument corrected, analyzed fluorescence spectra were plotted as 3d contour maps in MATLAB, with excitation wavelengths of 240 to 450nm and emission wavelengths of 300 to 600nm. Coble (1996) identified fluorescent bands corresponding to common fluorophores, presented in the table below.

Major fluorescence bands for water, with notations used herein and nomenclature proposed by Coble (1996). Table adapted from Huguet et al. (2009).

Excitation	Emission	Compound type	Letter used by Coble
max. (nm)	max. (nm)		(1996)
330-370	380-480	Humic substances	С
230-260	380-480	Humic substances + recent	A
		material	
310-320	380-420	Autochthonous production	M
270-280	300-340	Protein-like material	В
	max. (nm) 330-370 230-260 310-320	max. (nm) max. (nm) 330-370 380-480 230-260 380-480 310-320 380-420	max. (nm) max. (nm) 330-370 380-480 Humic substances 230-260 380-480 Humic substances + recent material 310-320 380-420 Autochthonous production

4.3 Fluorescence Indices

Three fluorescence indices have been developed to assess the origin and degree of transformation of DOC, based on the presence and concentration of different fluorophores. These indices are the f450/f500 fluorescence index (McKnight et al., 2001), the humification index (Zsolnay et al., 1999), and the biological autochthonous index (Huguet et al., 2009). My project primarily focused on the humification index and the biological autochthonous index. Indices were calculated for both the BES data and the end-member analyses.

4.3.1 The humification index

The humification index (HIX) was developed by Zsolnay et al. (1999) to assess the degree of maturation, or humification, in soils. Huguet et al. (2009) applied this technique to study the degree of humification of DOC in fluorescent spectra. Humification is associated with an increase in the carbon to hydrogen ratio, with a resulting shift to longer emission wavelengths (Huguet et al., 2009). This shift is associated with increasing aromaticity – higher HIX values correspond to the increased presence of complex, higher weight aromatic molecules. This index is calculated as the ratio H/L of two spectral regions in the spectra at $\lambda_{\rm exc} = 254$ nm. These two areas are calculated between $\lambda_{\rm em}$ s 300nm and 345nm for area L, and between $\lambda_{\rm em}$ s 435nm and 480nm for area H.

High HIX values (between 1 and 1.6) correspond with strongly humified and mature material, and lower values are associated with autochthonously produced DOC (Huguet et al., 2009; Zsolnay et al., 1999).

4.3.2 The biological autochthonous index

Huguet et al. (2009) introduced the biological autochthonous index (BIX) to determine the relative presence and contribution of the β fluorophore. This fluorophore is characteristic of

autochthonous biological activity in water samples, and its calculation is based on the expansion of the emission spectrum at $\lambda_{\rm exc}$ =310nm due to the presence of the β fluorophore. At $\lambda_{\rm exc}$ =310nm, the fluorescence intensity at $\lambda_{\rm em}$ =380nm - corresponding to the maximum fluorescence intensity of the isolated β fluorophore - by the fluorescent intensity at $\lambda_{\rm em}$ =430nm, the maximum intensity of the isolated α fluorophore, which corresponds with humic substance fluorescence. A higher BIX value is related to an increase in the concentration of the β fluorophore: BIX values >1 correspond to autochthonous DOC and the presence of DOC freshly released into the water. BIX values between 0.6 and 0.7 correspond to lower DOC production in natural waters (Huguet et al., 2009).

4.4 Parallel Factor Analysis

Parallel factor analysis, commonly known as PARAFAC, is a mathematical procedure that helps identify various fluorophores in EEMS. The procedure is a generalization of principal component analysis (PCA) to higher order arrays, with some differences. PARAFAC does not suffer from a rotational problem - pure spectra can be recovered from multi-way spectra data. One cannot, as in PCA, successively estimate components as this gives a model with worse fit than if the simultaneous solution is estimated. Furthermore, whereas PCA typically only keeps the first few components in the data accounting for the majority of the variance, PARAFAC generally keeps all identified components. An advantage is that the estimated models are mathematically simpler, making the resultant models simpler to interpret (Stedmon and Bro, 2008).

The procedure takes three-dimensional EEMs, and orthogonalizes the dataset to an alternate coordinate system, allowing for the identification of components, or fluorophores, that account for the majority of the variance in the data. In short, the model identifies components with characteristic emission and excitation wavelengths, with corresponding fluorescence intensities. The general equation for PARAFAC is

$$x_{ijk} = \sum_{f=1}^{F} = a_{if}b_{jf}c_{kf} + \epsilon_{ijk} \tag{1}$$

where $x_{textijk}$ is the fluorescence intensity of sample i measured at emission j and excitation k. The final term ϵ is the unresolved signal – residuals containing noise or error. The outcomes of the technique are the parameters a, b, and c, representing the concentration, emission spectra, and excitation spectra of identified fluorophores, respectively (Stedmon and Bro, 2008). PARAFAC was conducted on forty one total BES samples; as the robustness of the model depends on the number of spectra analyzed, PARAFAC modeling was not done for the end-member sources.

First and second order Rayleigh scatter peaks were removed from the data, and all data points above the peaks were removed. To account for the data points removed from the second order Rayleigh scatter, only emission wavelengths below 500nm were considered in the analysis. None of the common fluorophores identified by Coble (1996) have maximum intensities above $\lambda_{\rm em}=480{\rm nm}$.

5 Results and discussion

5.1 End member EEMs

Figures four, five, and six are compilations of all end-members EEMs over time. On all contour plots, $\lambda_{\rm exc}$ s 240 to 450nm plotted on the x-axis, and $\lambda_{\rm em}$ s 300 to 600nm on the y-axis. Intensities are plotted as Raman units (R.U.) on the *jet* colorscale, with blue being minimum fluorescence and red being maximum fluorescence.

From visual inspection, the sewage samples display three primary components: two components across $\lambda_{\rm em}=450{\rm nm}$ corresponding with the α' fluorophore identified by Coble (1996), indicating the presence of humic substances ($\lambda_{\rm exc}=360{\rm nm}$) with recent additions ($\lambda_{\rm exc}=270{\rm nm}$). The third fluorophore is located at $\lambda_{\rm exc}=270{\rm nm}$, $\lambda_{\rm em}=350{\rm nm}$, and corresponds with the γ fluorophore, indicating the presence of protein-like material. The location of the maximum fluorescence intensity also changes over time: in the fall, the maximum intensity corresponds with the α fluorophore, the γ fluorophore in the winter, and all three fluorophores in the spring.

Runoff samples have a single prominent fluorophore, also across $\lambda_{\rm em}$ =450nm and corresponding with the α' fluorophore. The location of the maximum fluorescence intensity does not change over time, although maximum intensity varies.

Algae has one primary fluorescent compound corresponding to the γ fluorophore, with a minor α peak during the fall. This is surprising, as I expected the primary fluorophore to be attributed to autochthonous production, rather than proteins. It is possible that by trying to isolate algae contributions by drying then releaching, I may have halted the metabolism of the algae.

Leaf litter from Oregon Ridge exhibits a single major α peak in the fall, but expands into three components in the winter, with a distribution similar to that of sewage. Fall leaf litter from Gwynns Run and Dead Run display similar α -like peaks in the fall, and like leaf litter from Oregon Ridge, shifts to a three component plot in the winter. The slightly different starting fluorophores for all three groups of leaf litter in the fall eventually converge to a similar fluorescence distribution in the winter. This is likely due to bacterial metabolism breaking down readily available organic compounds in the leaf litter over time.

The last end-member EEM is that of the soil sample collected from Dead Run during winter sampling. Only one sample was collected as 2012 was a particularly dry year, and the DOC composition of deeper soil was not expected to vary greatly on a seasonal basis. Two fluorophores are identifiable – a γ peak and an α' peak. The optical space occupied by mature, humic substances was not very fluorescent. This suggests that either soil DOC turnover at Dead Run is relatively high, or that my sample was not collected at a deep enough depth. The maximum fluorescence of this soil sample lie slightly outside of the constrained optical space, into wavelengths where the Xenon lamp of the spectrofluorometer is less accurate.

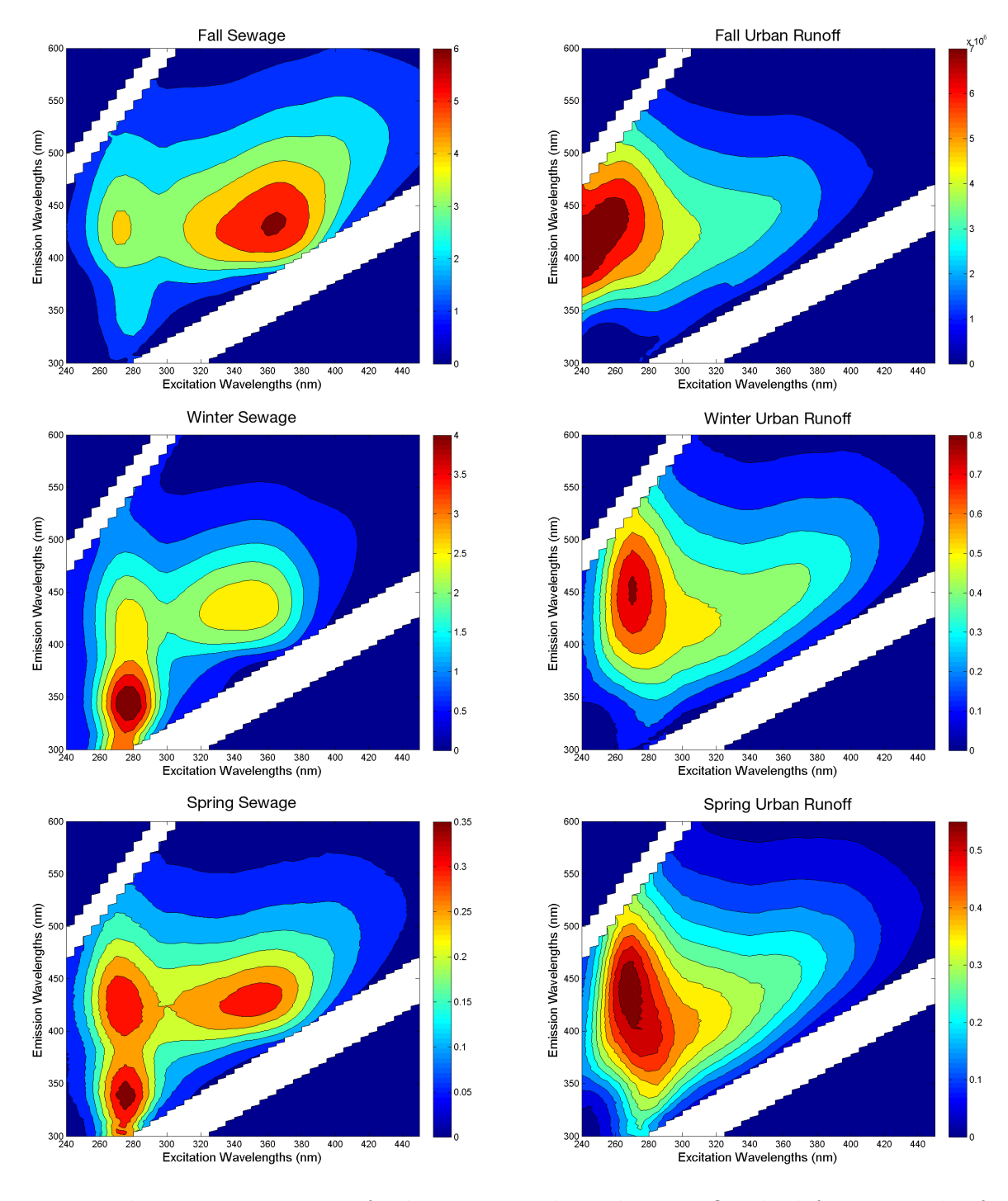


Figure 4: Fluorescence spectra of urban sources through time. On the left are samples from the Back River Sewage Plant, and on the right are stormwater runoff samples collected from the storm drain below I-93 at Carroll Park.

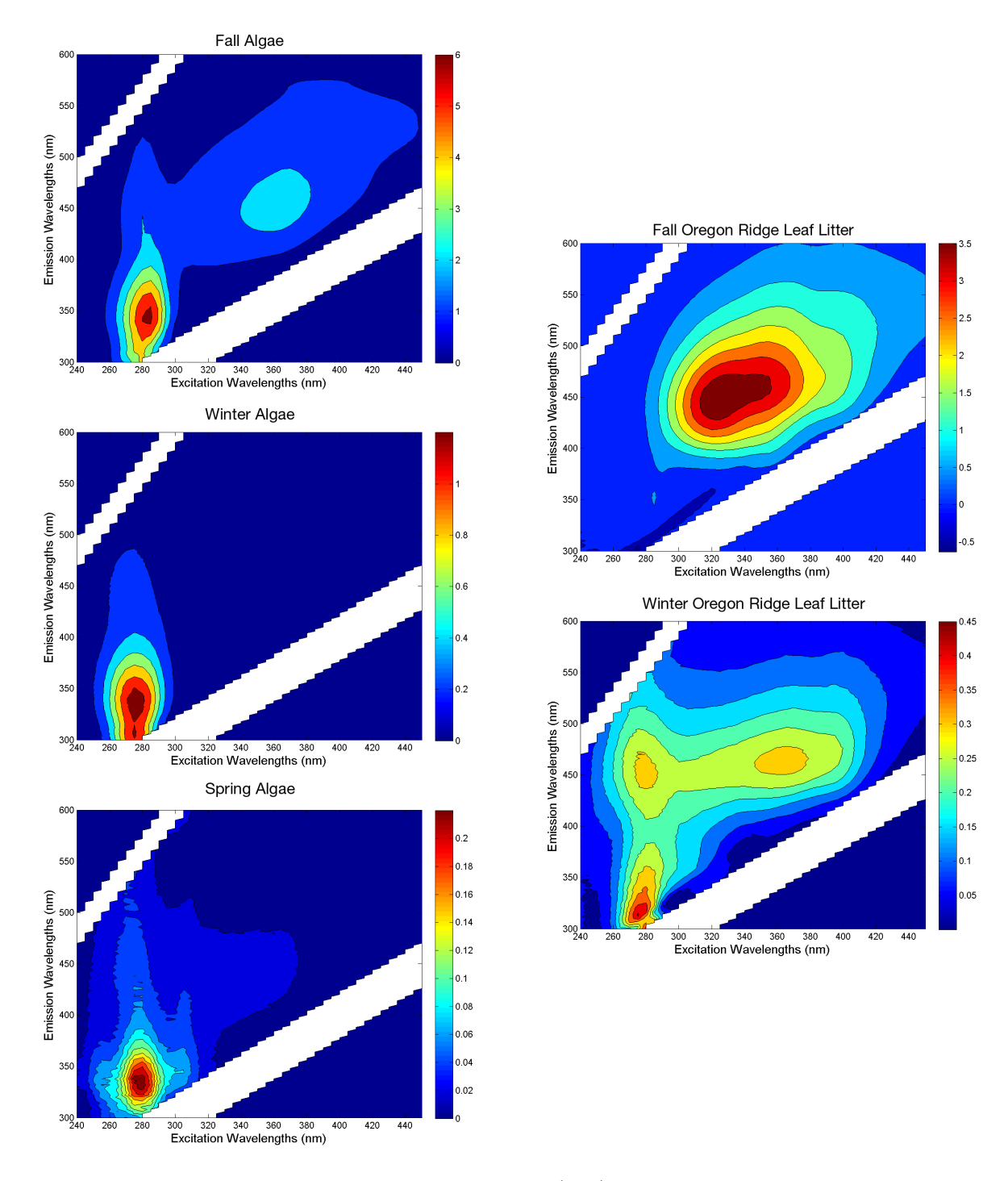


Figure 5: Fluorescence spectra of algae samples (left) and leaf litter samples from Oregon Ridge (right).

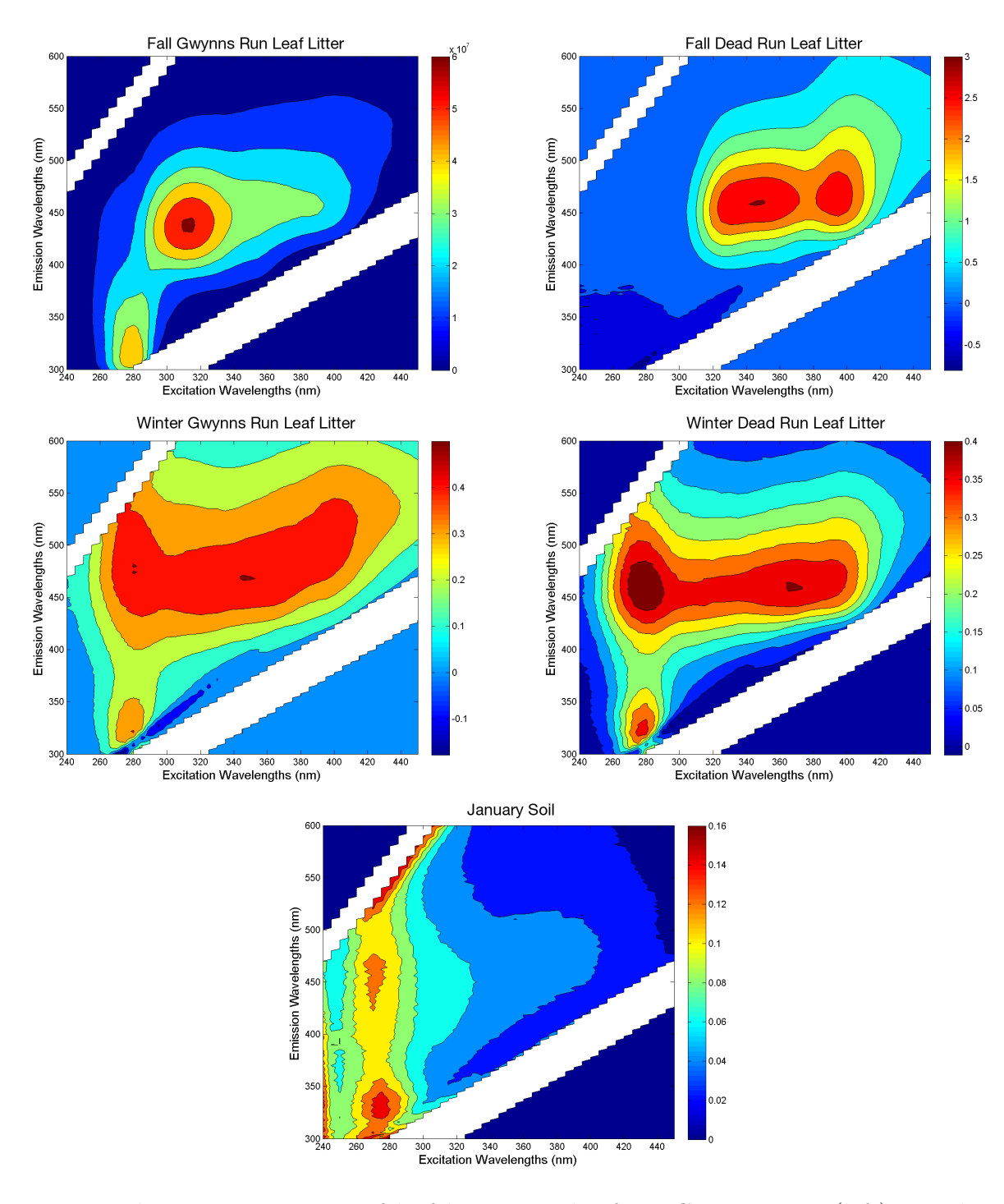


Figure 6: Fluorescence spectra of leaf litter samples from Gwynns Run (left), Dead Run (right), and soil from Dead Run (bottom).

5.2 Fluorescence Indices

Humification index (HIX) and biological autochthonous index (BIX) values were plotted in a variety of formats. Figure 7 is a compilation of HIX and BIX values for all four BES streams over time.

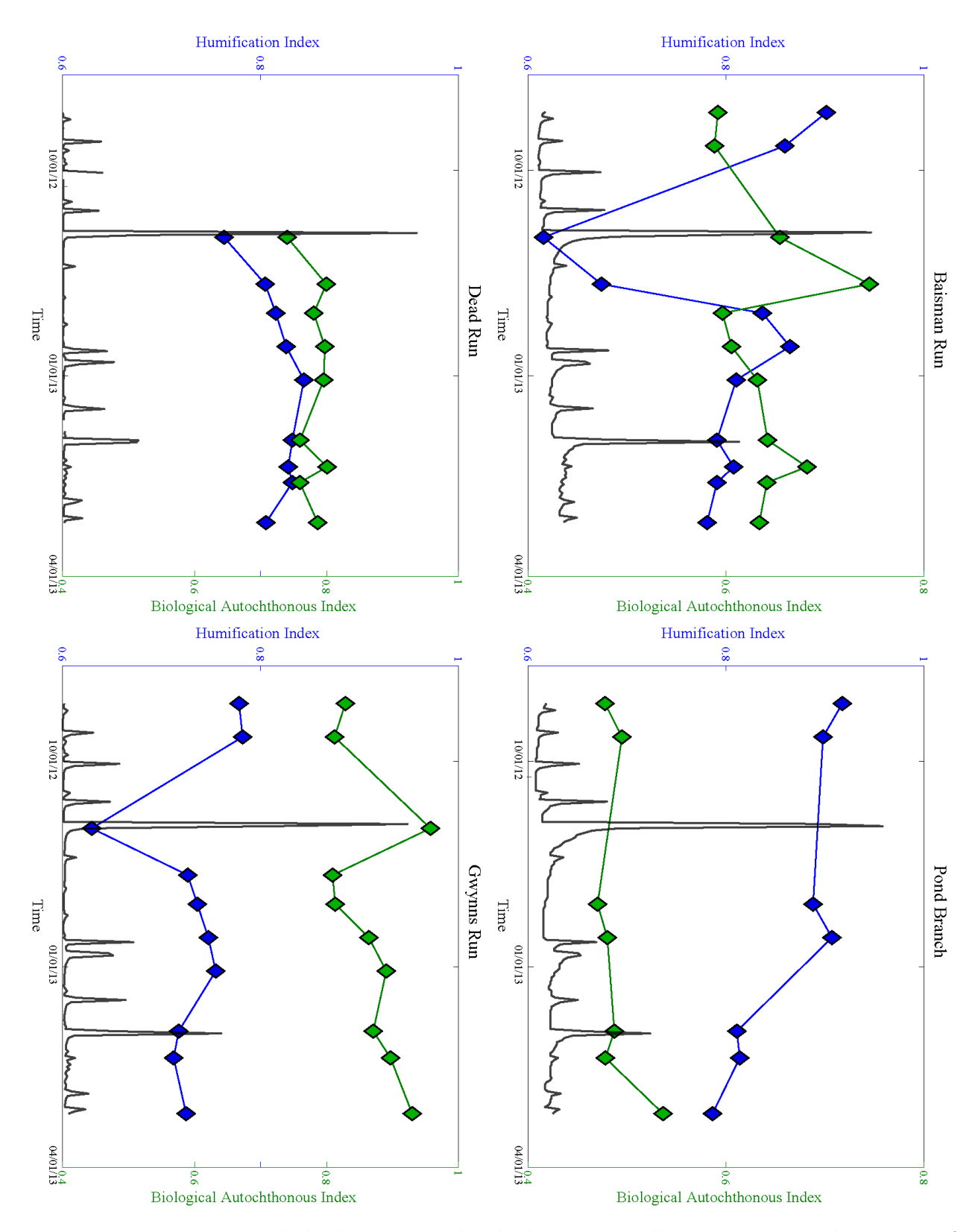


Figure 7: HIX, BIX, and discharge at individual sites. Discharge is measured in units of cubic feet per second. Error bars not plotted as analytical uncertainty for the calculation of each index did not exceed 2% for HIX, and 1% for BIX.

Discharge is superimposed atop the index values in dark gray, plotted on the same time scale. Discharge for Gwynns Run was estimated from discharge at Carroll Park, and the large spike in discharge in late October coincides with Hurricane Sandy. Gaps in data can be attributed either to sampling gaps, or samples identified as anomalous by PARAFAC. Four samples were identified as anomalous by PARAFAC – samples on 10/31/2012 and 11/21/2012 from Pond Branch, and samples on 09/05/2012 and 09/05/2012 from Dead Run. Notably, the 10/31/2012 Pond Branch sample was the sample taken directly after Hurricane Sandy. The analytical uncertainty for the calculation of each index did not exceed 2% for HIX, and 1% for BIX. Error bars were not plotted as the uncertainty associated with each calculation are smaller than the resolution allowed on the plots.

Two relationships are apparent. The first is that HIX and BIX are negatively correlated (r = -0.68, p < 0.05) - BIX increases as HIX decreases, and vice versa . Secondly, HIX and BIX values are tied to discharge. As discharge increases, HIX values decrease and BIX values decrease. This is most readily apparent at the large peak in discharge observed at all sites at the end of October, corresponding to Hurricane Sandy. The biweekly resolution of sampling is insufficient to resolve lag time between changes in HIX/BIX, unfortunately. Figure 8 is a plot of all available HIX and BIX data against discharge on a logarithmic scale. Although there is some scatter, the overall trend is that HIX decreases with increasing discharge, and BIX increases with increasing discharge. Both relationships have p < 0.05.

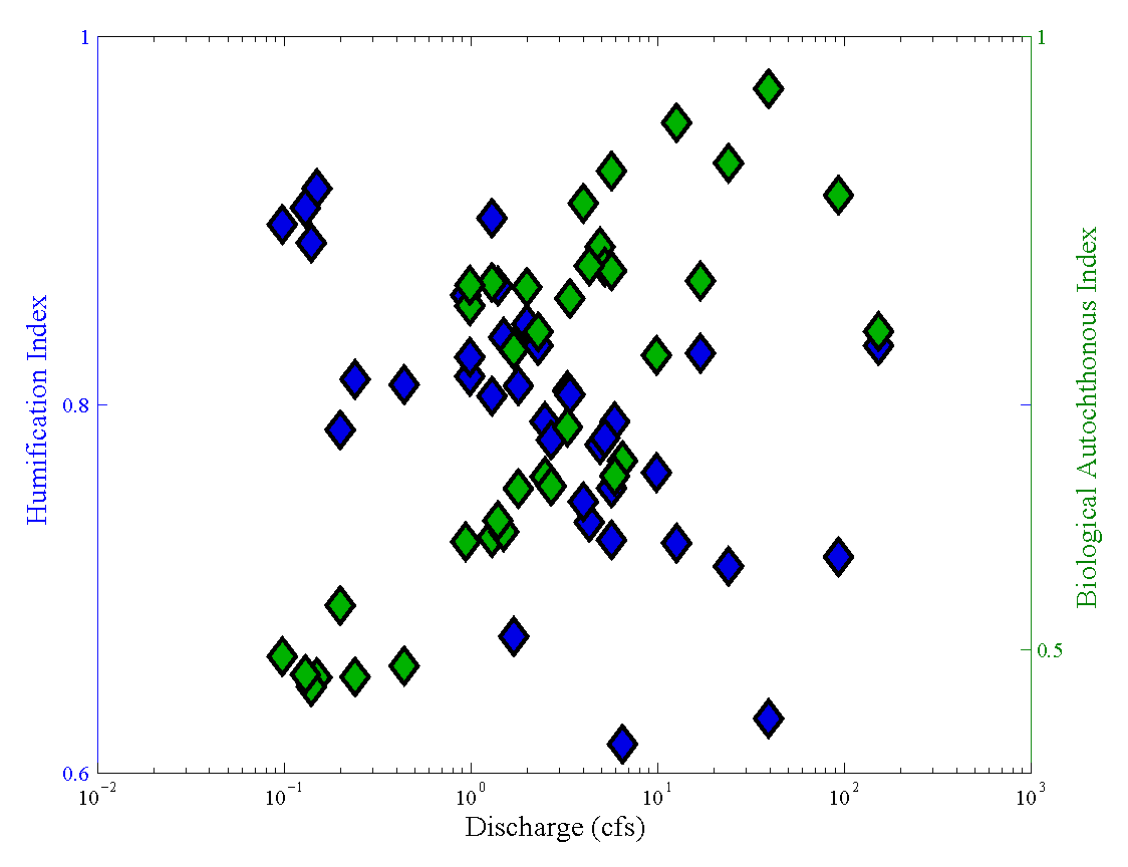


Figure 8: HIX and BIX plotted as a function of discharge on a logarithmic scale. Error bars not plotted as analytical uncertainty for the calculation of each index did not exceed 2% for HIX, and 1% for BIX.

None of the BES streams exhibited extreme HIX/BIX values, indicating that none of the streams had DOC sourced entirely from either humified DOC or from biologically produced DOC. Next, figure 9 is a plot of both BES data and end-member data index data on the same plot, with BIX on the y-axis as a function of HIX.

Although not evident in visual inspection of their EEMs, the algae samples have very low HIX values and elevated BIX values, consistent with elevated biological productivity.

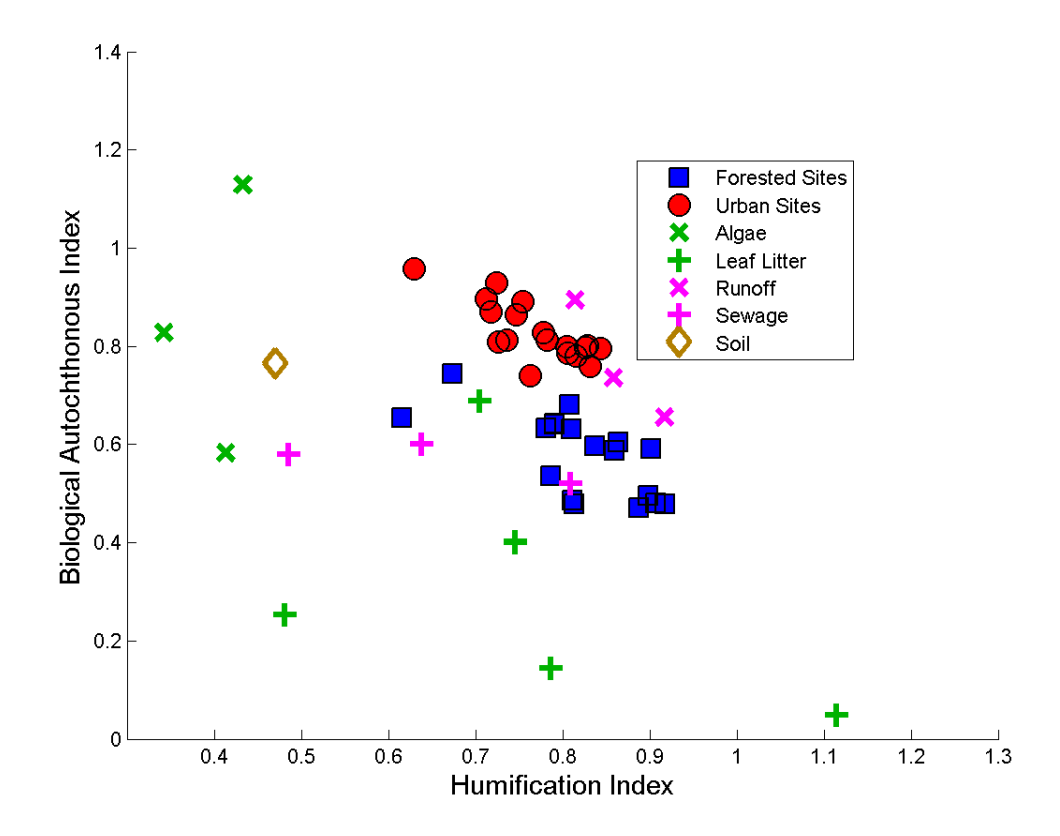


Figure 9: BIX plotted as a function of HIX across all sites. Error bars not plotted as analytical uncertainty for the calculation of each index did not exceed 2% for HIX, and 1% for BIX.

The leaf litter samples progressed to higher HIX values over time, consistent with the development of α' peaks in the EEMs over time. Soil index values plotted between algae and the BES sites.

Sewage samples plot in relatively the same area as the forested streams and the stormwater runoff samples plot similarly to the urban streams. Though it is unlikely that these two end-members are the sole sources of DOC to streams, this provides a starting point for analyzing DOC sources. Urbanized streams have higher drainage densities and impervious surfaces than forested streams and consequentially, have higher inputs from surface runoff than forested streams. Storm drains in Baltimore drain directly from the streets, and the end-member spectra of stormwater runoff is a good approximation of DOC associated with urban runoff.

Kaushal and Belt (2012) observed that the forested streams located in Oregon Ridge State Park are situated next to residential developments and septic systems. The similarity of the HIX/BIX values of the sewage to the forested streams may suggest inputs from leaking or aging septic systems.

This suggests a hydrological control on sources of DOC to these streams. Increases in stream discharge reflect immediate increases in precipitation and surface runoff. Increased precipitation would result in addition of nutrient and pollutant-rich water to the streams, stimulating autochthonous production. At the same time, this water would have less contact with more humified and "mature" sources of organic carbon, resulting in a suppression of the HIX. Delayed input from groundwater in contact with deeper, older soils may explain the rise in HIX after a storm event. As observed, forested streams have slightly higher HIX values than urban streams, and urban streams have higher BIX values than forested streams.

5.3 PARAFAC results

The PARAFAC model identified the same three components in the urban and forested streams (Figure 10), accounting for 99.3% and 99.6% of the variance in the data, respectively. The first two components in both systems are the same. The first component in forested streams and the second in urban streams (figure 10a,10e) is similar to a terrestrial reduced quinone-like component (SQ1) identified by Cory and Mcknight (2005), but it more closely resembles a mixture of α and α' fluorophores. The second component in forested streams and first in urban streams (10a, 10d) corresponds to humic substances with recent additions, the α' fluorophores identified by Coble (1996), The third component is the γ fluorophore, indicating the presence of proteins and amino acids, identified in figure 10c and 10f.

While the same three components were identified in both sets of data, the relative contributions of each varied. In forested streams, the dominant fluorophore was the more humified α fluorophore, and the dominant fluorophore in urban streams the α' . This is consistent with the proposed hydrological control on DOC, as the dominance of the α' fluorophore in the urban streams suggests quicker turnover of DOC in the streams due to higher stream discharge. Moreover, recall that the end-member spectra of stormdrain runoff exhibited fluorescence primarily from the α' fluorophore and that the HIX/BIX values of runoff plotted very similarly to the HIX/BIX values of the urban streams.

DOC sources to the forested streams are harder to constrain. While the dominant component is the humified α fluorophore, both leaf litter and sewage spectra exhibited prominent α fluorophore peaks. Kaushal and Belt (2012), however, discovered that stream samples in Oregon Ridge exhibited elevated levels of dissolved nitrogen, consistent with elevated nitrogen levels found in sewage. This, combined with the similarity of the HIX/BIX values of sewage to the forested streams suggests that these streams may be receiving a sizeable amount of DOC from sewage.

Due to the ubiquitous presence of algae in both forested and urban streams and the optical characteristics of the algae spectra, the γ fluorophore present as the third component in both forested and urban streams is likely due to algae. The lack of a prominent autochthonous production component suggests that all four streams are heterotrophic in nature, rather than autotrophic.

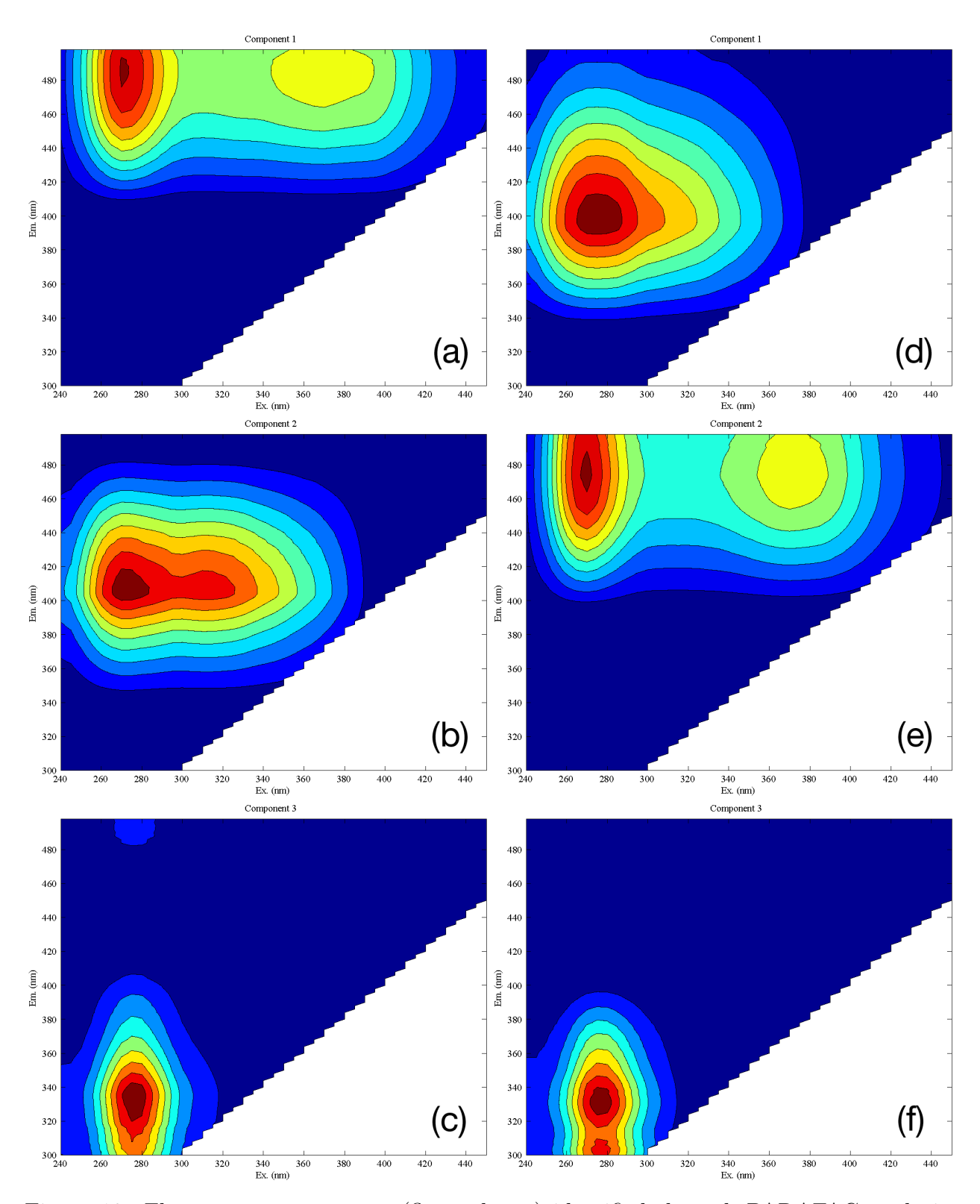


Figure 10: Fluorescent components (fluorophores) identified through PARAFAC analysis. (a), (b), and (c) are forested components in descending order of relative contribution, and (d), (e), (f) are urban components in descending order of relative contribution.

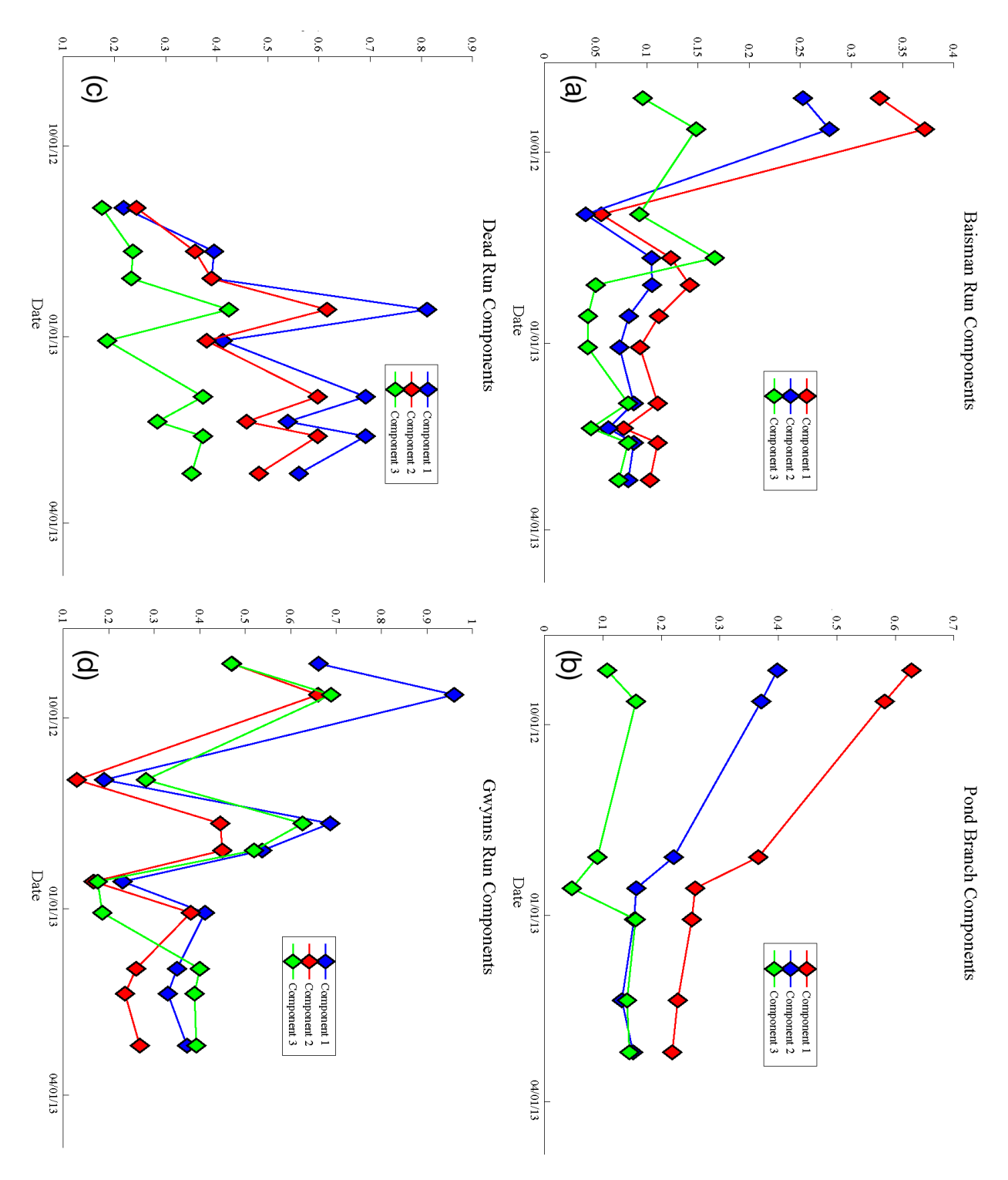


Figure 11: Fluorescent components (fluorophores) identified through PARAFAC analysis. (a), (b), and (c) are forested components in descending order of relative contribution, and (d), (e), (f) are urban components in descending order of relative contribution.

Lastly, I plotted the components identified by PARAFAC over time for each BES stream. The three lines - red, blue, and green - correspond to the same components identified in both the urban and forested sites: the red line is the α fluorophore, the blue line is the α' fluorophore, and the green line is the γ fluorophore. α and α' component loadings are highest in the fall, consistent with DOC inputs from decaying leaf litter. Unlike the plots of HIX/BIX as a function of discharge, all three components follow the same general pattern: as one fluorophore increases or decreases, the others follow suit. This is likely tied to the maximum fluorescence intensity of the sample.

6 Directions for future work

The next step would be to expand these analyses to the summer, and perhaps into another year. Further work should be done to identify the component loadings in each end-member source via PARAFAC over time: providing a model of the fluorophores present in each end-member source, and how they vary over time. Furthermore, these analyses should be complimented with synchronous total organic carbon (TOC) and total dissolved nitrogen (TDN) analyses.

As human population, urbanization, and pollution increase, urban water quality concerns become more apparent. Further research done to study the combined impacts of climate change and land use on streams can help inform policy makers on both local and regional scales. Better constraining both how DOC in urban streams and end-member sources vary may allow for a rapid way to identify organic pollutants such as sewage or polycyclic aromatic hydrocarbons in urbanized streams, aiding in restoration and remediation of urban streams.

7 Conclusions

Dissolved organic carbon (DOC) is a heterogeneous amalgamation of compounds that serves as the basis of heterotrophic aquatic systems. However, an excess of DOC in a riverine system may be detrimental to ecosystem and human health as it contributes to freshwater acidity, facilitates downstream pollutant transport, and in extreme cases, contributes to watershed eutrophication. While interest in DOC has increased in the past two decades, little work has been done on the combined impacts of climate change and land use on urban watersheds, and even less work has been done on studying anthropogenic contributions of DOC to urban watersheds. Using a combination of excitation-emission-matrics (EEMs), fluorescence indices, and PARAFAC, my project identified potential sources of DOC to four Baltimore area streams.

My results are consistent with my first hypothesis – anthropogenic and natural sources of DOC can be identified and differentiated with fluorescence spectroscopy. Differences not immediately apparent from visual analysis of EEMs can be resolved through the use of fluorescence indices and PARAFAC.

7.1 Potential for tracking natural vs. anthropogenic sources of DOC in streams

I found that optical properties show the potential for identifying sources of DOC. Some end-member sources of DOC were readily identifiable by their optical characteristics (algae, stormwater runoff), while others (sewage, humified leaf litter) were not. In the case of the latter, a better understanding can be gained through the application of fluorescence indices, primarily the humification index (HIX) and the biological autochthonous index (BIX). These indices measure the degree of maturation, or humification, of a sample and the degree of biological autochthonous production, respectively, in an EEM. A combination of these two techniques may allow for a rapid, and relatively in-expensive way of preliminary identifying organic pollutants in urban watersheds.

Combining these techniques with total organic carbon (TOC) and other nutrient analyses may provide a more accurate characterization of DOC sources in an watershed. As an example, Kaushal and Belt (2012) recognized the presence of residential developments adjacent to Oregon Ridge State Park, and measured high nitrogen levels in the park's streams, corresponding to the high nitrogen levels typically found in sewage. Combined with my work done with fluorescence indices and PARAFAC, this suggests that streams in the area may be receiving inputs of organic carbon from ageing septic systems.

Work done by Hudson et al. (2007) also looked at the fluorescence characteristics of sewage, but the study was conducted in England and did not apply fluorescence indices nor PARAFAC to their results. To the best of my knowledge, this study is relatively novel in its combination of EEM-PARAFAC with fluorescence indices; all three techniques have been used and extensively published on previously, but none have combined all three techniques.

7.2 Hydrologic variability drives sources and quality of DOC exported to streams

Streamflow strongly influenced the sources and quality of DOC. Higher discharge rates resulted in a suppression of the HIX and an increase in BIX. Urban streams, which have higher discharges than forested streams due to the development of urban infrastructure, consistently had higher BIX values than their forested counterparts. In our area, this is exacerbated by the prevalence of high flow events such as hurricanes and snowmelt events. An example of this can be seen in figure 7, where the large discharge event associated with Hurricane Sandy caused a large decrease in HIX and a corresponding increase in BIX. However, fluorescence data was only available four days after peak discharge - it is possible that what is recorded in my data is a reflection of the immediate aftereffects of a high flow event: increased Hortonian overland flow, leading to a short term influx of water rich with recently humified organic carbon, stimulating biological production. The increased flow rates would also result in water with less contact with older, more humified substances. The return of HIX values to more "baseline" values may be due to groundwater recharge. This is consistent with Yamashite et al. (2008), who also concluded that the distribution of terrestrial humic-like substances are strongly controlled by riverine inputs.

7.3 DOC components in forested and urban streams

Three components were identified with PARAFAC for both forested and urban streams – each explaining over 99% of the variance present in the data. These components shared the same optical characteristics, consistent with my null hypothesis. However, the components differed in their relative contribution to the overall variance in the data set. Forested streams experienced more input from more mature and humified sources of DOC, while urban streams experienced quicker DOC turnover, with more input from recently humified material.

The first two components identified for both systems (the α and α' fluorophores) are suggested to have a terrestrial, allochthonous origin, in line with previous work done (Coble, 1996; Yamashita et al., 2008; Cory and McKnight, 2005). The third component (γ fluorophore) is associated with autochthonous origin (Coble, 1996; Yamashita et al., 2008) and may be biologically labile. This study is consistent with past work that allochthonous and autochthonous origins of DOC can be distinguished in urban streams through the use of fluorescence indices, and EEM-PARAFAC, suggesting that fluorescence spectroscopy is important for better evaluation and understanding of DOC dynamics in riverine systems.

8 Acknowledgements

This research was supported by grantsfrom the National Science Foundation (NSF) LTER program (NSF DEB-9714835 and 0423476), NSF DBI 0640300, NSF CBET 1058502, Maryland Sea Grant SA7528085-U, Maryland Sea Grant NA05OAR4171042, Maryland Sea Grant R/WS-2, and NASA NNX11AM28G. I would like to thank Sujay Kaushal in being patient and supportive of me, Rose Smith and Tom Doody for being invaluable to sample collection, and the rest of the Kaushal lab. Comments from Jill Cleveland and Kristin Benke were also invaluable for writing the fluorescence section of my thesis. Lastly, I would also like to thank beer for always being there when I needed it, and coffee for keeping me awake, even to the very bitter end.

Bibliography

- Boesch, D.F., E. Burreson, W. Dennison, E. Houde, M. Kemp, V. Kennedy, R. Newell, K. Paynter, R. Orth, and W. Ulanowicz, 2001. Factors in the decline of coastal ecosystems. Science 293:629–638. doi:10.1126/science.293.5535.1589c.
- Boyer, J.N., P. M. Groffman, 1996. Bioavailability of water extractable carbon fractions in forest and agricultural soil profiles. Soil Biology and Biochemistry 28, p. 783-790. doi: 10.1016/0038-0717(96)00015-6
- Cory, R. M., and D. M. Mcknight, 2005. Fluorescence spectroscopy reveals ubiquitous presence of oxidized and reduced quinones in dissolved organic matter. Environmental Science and Technology. 39:8142-8149.
- Doney, S. C., V.J., Fabry, R. A., Feely, J. A., Kleypas, 2009. Ocean Acidification: The Other CO2 Problem. Annual Review of Marine Science, v. 1, p. 169-192.
- Doney, S. C., 2010. The Growing Human Footprint on Coastal and Open-Ocean Biogeochemistry. Science, v. 328, no. 5985, p. 1512-1516.
- Findlay S. & Sinsabaugh R.L. (1999) Unravelling the sources and bioavailability of dissolved organic matter in aquatic ecosystems. Marine and Freshwater Research, 50, 781-790.
- Findlay, S., J. M., Quinn, C. W. Hickey, G. Burrell, M. Downes, 2001. Effects of Land Use and Riparian Flowpath on Delivery of Organic Carbon to Streams. Limn. And Oceano. v. 46, p. 345-355.
- Groffman, P. M., N. L., Law, K. T. Belt, L. E. Band, G. T. Fisher, 2004. Nitrogen Fluxes and Retention in Urban Watershed Ecosystems. Ecosystems 7, 393-403.
- Huguet, A., L. Vacher, S. Relexans, S. Saubusse, J.M. Froidefond, E. Parlanti, 2009. Properties of fluorescent dissolved organic matter in the Gironde Estuary. Organic Geochemistry 40, p. 706-719.
- Hudson, N., A. Baker, D. Reynolds, 2007. Fluorescence analysis of dissolved organic matter in natural, waste and polluted waters -- a review. River research and applications 23, p. 631-649.
- Kaushal, S.S. and W.M. Lewis, Jr. 2003. Patterns in the chemical fractionation of organic nitrogen in Rocky Mountain streams. Ecosystems 6: 483-492.
- Kaushal, S.S., P.M. Groffman, L.E. Band, C.A. Shields, R.P. Morgan, M.A. Palmer, K.T. Belt, G.T. Fisher, C.M. Swan, and S.E.G. Findlay. Interaction between urbanization and climate variability amplifies watershed nitrate export in Maryland. Environmental Science & Technology 42, 5872-5878, 2008. doi:10.1021/es800264f.

- Kaushal, S. S., K. T. Belt, 2012. The urban watershed continuum: evolving spatial and temporal dimensions. Urban Ecosystems 15, p. 409-435.
- Mcknight, D. M., E. W. Boyer, P. K. Westerhoff, P. T. Doran, T. Kulbe, D. T. Anderson, 2001. Spectrofluorometric characterization of dissolved organic matter for indication of precursor organic material and aromaticity. Limnol. Oceanogr. 46, p. 38-48.
- Ritchie, J. D., E. M. Boyer, 2003. Proton binding study of standard and reference fulvic acids, humic acids, and natural organic matter. Geochimica et Cosmochimica Act 67, p. 85-96.
- Skoog, Douglas A., F. James. Holler, and Stanley R. Crouch. *Principles of Instrumental Analysis*. 6th ed. Belmont, CA: Thomson Brooks/Cole, 2007. Print.
- Stedmon, C. A. and S. S. Markager, 2005. Tracing the production and degradation of autochthonous fractions of dissolved organic matter by fluorescence analysis. Linol. Oceanogr. 50, p. 686-697.
- Stedmon, C. A., R. Bro, 2008. Characterizing dissolved organic matter fluorescence with parallel factor analysis. Limnology and Oceanography: Methods, v. 6, p. 572-579.
- Yamashita, Y., R Jaffè, N. Maie, E. Tanoue, 2008. Assessing the dynamics of dissolved organic matter in coastal environments by excitation emission matrix fluorescence and parallel factor analysis (EEM-PARAFAC. Limnol. Oceanogr. 53, 1900-1908.

10 Appendix I

I pledge on my honor that I have not given or received any unauthorized assistance on this assignment/examination.

Grant Jiang